Instrument Report for Honeywell Atmospheric Winds Campaign for Space (HAWCS)

Authors: Kaizhong Gao, Ph. D., Patrick Conry, Ph. D., Erik Horak, Ph. D. and Thomas Dobbins, Ph. D.

Aerospace Technologies, Honeywell International, Inc., Plymouth, MN, USA

Contents

Table of Figures

Table of Tables

1. Executive Summary

The HALAS system has proven capable of delivering timely weather information from high-altitude atmospheric lidar measurements in both ground and aircraft-based variants. A space-based HALAS represents the next frontier for technological development that would expand the geographical footprint and benefit the earth observing network, while adding valuable data to the predictive modeling mission of NOAA. Modeling of a HALAS space-based system could achieve the requirements for 3D wind measurements from measuring the atmospheric wind profile: Call for Studies and Field Measurement Campaigns Broad Agency Announcement (BAA-NOAA-3DWinds-2022).

The modeling study indicated that technological changes are recommended for a successful HALAS space-variant, most importantly a detector with minimal background noise. A 3D wind measurement from a lidar requires 3 or more lines-of-sight (LOS), and several strategies are proposed: multiple satellites, multiple telescopes, a single telescope continuously moving about the nadir, and a combination thereof. Size, weight, and power (SWAP) estimates for a HALAS space-variant capable of 3D Wind Measurement were benchmarked against the European Space Agency's (ESA) Aeolus-1 satellite. In comparison to Aeolus-1, the HALAS space-variant SWAP estimation concluded that the scientific payload could be significantly reduced in volume with slight reduction in mass and further reductions were possible. The key technical challenges to achieve a BAA-NOAA-3DWinds-2022 performant wind measurement with a HALAS space-variant are discussed along with the ongoing, planned, and proposed technological improvements. Overall, a potential HALAS space-variant can achieve the BAA-NOAA-3DWinds-2022 minimum requirements with a reduced SWAP compared to the Aeolus-I satellite but will require investment to achieve the required technological enhancements, engineering SWAP, and ruggedization for the space environment.

2. Introduction to HALAS

2.1 HALAS Working Principle

The HALAS system operates based on Light Detection and Ranging (LiDAR) technology. A high-powered pulsed laser is emitted into the sky. As this laser pulse traverses the atmosphere the laser light interacts with various particles in the atmosphere such as aerosols (dust, water droplets, etc.) and molecules (nitrogen, oxygen, etc.). This interaction results in several types of scattering. A small portion of the scattered light is backscattered and harvested by a telescope coaligned with the laser. The collected backscattered light carries information about various atmospheric physical properties including temperature, density, humidity, wind vector, and others. Retrieval of these atmospheric data products is done through careful optical interrogation of the backscattered light and post-processing of the signal responses on multiple detectors.

Three key features of LiDAR technology make HALAS an attractive, powerful weather measurement platform.

The pulsed laser nature of the measurement allows for a time-of-flight detection of the backscattered light allowing for range/altitude resolved atmospheric data product retrieval. Said another way, as the laser pulse traverses the atmosphere at the speed of light, it scatters off atmospheric constituents at different altitudes at subtly different times. The backscattered light is measured as a function of time, which is related to a range ($range = time \times speed\ of\ light/2$), and can in turn be related to an altitude. This results in backscattering as a function of altitude allowing for retrieval of atmospheric data products as a function of altitude.

The parallel sensing of different optical properties of the backscattered light by separate optical instruments allows for all the above-mentioned atmospheric data products to be collected simultaneously from a single HALAS measurement. A more detailed description of the optical characteristics of the backscattered light and the instrumentation to measure them will be in the following sections.

The atmosphere is measured along the trajectory of the laser pulse. This allows for a highly localized and repeatable measurements location. Additionally, the line of sight of the laser can be changed to direct the atmospheric measurement to target a particular area of interest.

Together HALAS measurements provide a localized, repeatable, simultaneous measurement of the key altitude-resolved atmospheric properties.

2.2. Types of Atmospheric Scattering

The atmospheric information carried by the backscattered light is found in the optical characteristics of the light. Broadly, there are two types of scattering collected: elastic and inelastic. The elastic scattering of light occurs at approximately the same wavelength as the laser light that was transmitted through the atmosphere. The inelastic scattering light occurs at a different wavelength than the laser light. In the case of HALAS, where a 355 nm UV laser is transmitted into the atmosphere, the return light that is approximately 355 nm (change of <<1 nm,

~0.001 nm) is elastically scattered return whereas light with a wavelength change >0.1 nm (and up to >70 nm change) is inelastically scattered light.

The physical process for generating elastic and inelastic scattering varies with elastic scattering originating in Rayleigh and Mie scattering, whereas inelastic scattering originates from Raman scattering with both rotational Raman and Vibrational Raman scattering collected. Each scattering process plays an important role in HALAS technology seen in Figure 1. Specifically, Mie scattering provides information about aerosol properties including scattering (aerosol extinction), bulk speed (wind), and presence (cloud height). Rayleigh scattering provides information about molecular properties including scattering (molecular scattering), quantity (molecular density), and bulk speed (wind). Rotational Raman scattering provides information about molecular rotational speeds (molecular temperature). Vibrational Raman scattering provides information about quantities of individual molecular quantities, most importantly water vapor quantities (humidity).

Figure 1: Types of Atmospheric Scattering Collected in HALAS Measurements.

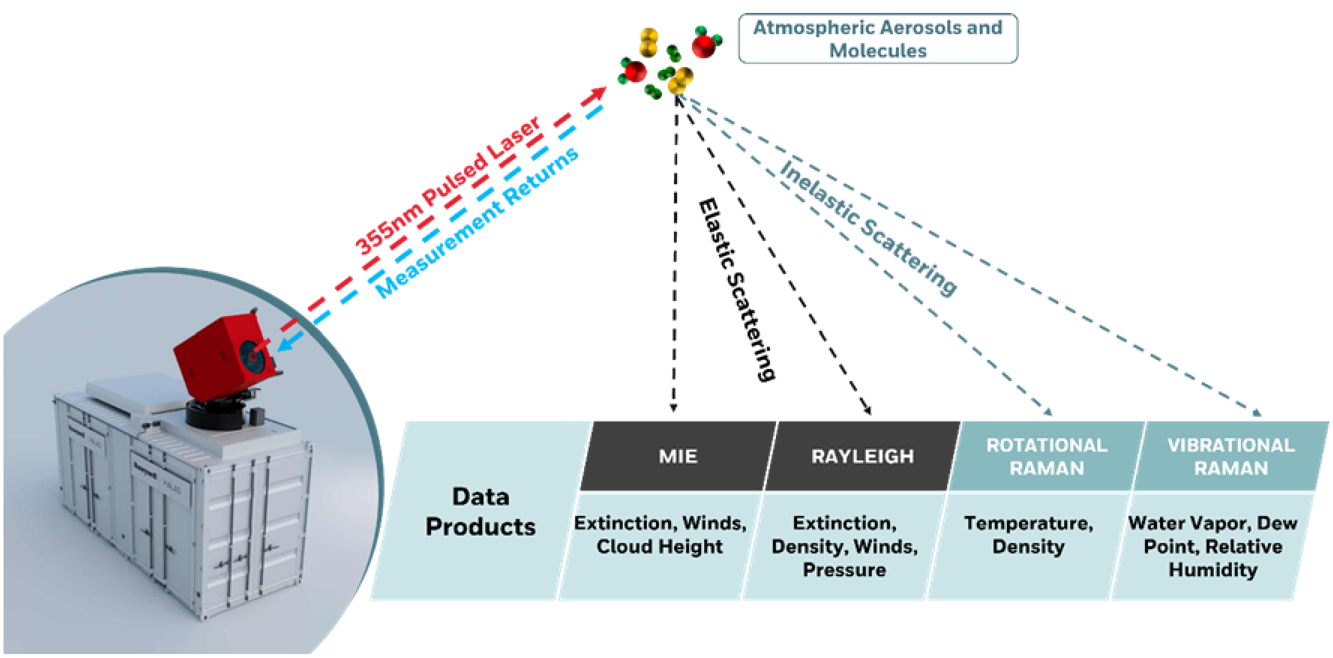

Further, additional details can be gleaned through further examination of individual scattering returns and through combined analysis of multiple scattering properties.

2.2.1. Mie Scattering

Mie scattering occurs when light interacts with aerosols (water droplets, dust, pollen, smoke, etc.). These particles are typically larger or comparable in size to the wavelength of the scattered light. This phenomenon is named after the German physicist Gustav Mie, who developed the theory in 1908. While the original theory is limited to spherical particles interacting with an electromagnetic plane wave, more general particle makeup (size, shape, composition, etc.) with a more general optical field can readily be understood by extended theories and computer simulations. While the specific scattering response both in intensity and angular dependence is complex, some general implications are readily understood.

- Mie scattering is much stronger than other forms of scattering. This means that elastic scattering in an aerosol-rich environment is dominated by Mie scattering and not Rayleigh scattering. The scattering strength under certain conditions (e.g., clouds, fog, smoke) can be strong enough to limit transmission through the atmosphere. A good rule of thumb is if atmospheric conditions are such that an observer cannot see through them, then UV LIDAR technology will also not be able to.

- Mie scattering angular dependence is extraordinarily complex. The amount of backscattered light to total scattering can vary dramatically depending upon the precise aerosol identity. This is important as the collected LiDAR signal is dependent on the backscattering signal while the extinction/attenuation through the atmosphere is related to the total scattering value.

- Mie scattering can have non-trivial polarization responses. While scattering from spherical particles does not alter the incident polarization, non-spherical particles can strongly alter the polarization.

This Mie scattering information is used strategically in HALAS technology to determine atmospheric properties. The location and intensity of the Mie scattering provide direct information about aerosol loadings. For example, the cloud presence and cloud height (altitude) are readily determined by the amount of Mie scattering. The amount of Mie scattering can also yield extinction coefficient through the atmosphere. In addition, because Mie scattering contributes to wind measurements the increased intensity from aerosols can improve wind measurements.

2.2.2. Rayleigh Scattering

Rayleigh Scattering, named after the British physicist Lord Rayleigh, occurs when light interacts with objects much smaller than the wavelength of light. Rayleigh scattering in the atmosphere primarily occurs with molecules (nitrogen, oxygen, water vapor, etc.), providing critical information about the molecular content of the atmosphere. Unlike Mie scattering, Rayleigh scattering provides a highly predictable atmospheric response with general implications listed below.

- Rayleigh scattering has a strong wavelength dependence with a $1/\lambda^4$ dependence. This has strong implications for the choice of wavelength chosen in the HALAS technology, with a UV wavelength chosen as it increases the Rayleigh signal strength. Specifically, the 355 nm wavelength provides a 5x molecular scattering strength relative to 532 nm and an 80× improvement compared to 1064 nm. Despite this signal increase Rayleigh scattering from molecules is a very weak phenomenon requiring a high-power laser and/or a large telescope to detect a reasonable amount of signals.

- Rayleigh scattering has a simple angular dependence with a symmetric and well-understood relationship. This allows for a known relationship between backscattering and total scattering to yield the known relationship between signal and attenuation/extinction from atmospheric molecular components.

- Rayleigh scattering has a simple polarization response. The molecules do not change the incident polarization.

Importantly, the highly predictable nature of the Rayleigh scattering makes it an important part of the atmospheric property calculation. The intensity is readily converted into molecular concentration or density. Likewise, scattering can be used to calculate molecular extinction through the atmosphere. Additionally, Rayleigh scattering carries wind information. Importantly, unlike aerosol loadings which are highly dependent upon local atmospheric conditions, molecular concentrations are highly reliable with altitude providing consistent signal intensity in certain atmospheric conditions when not overly dampened by Mie scattering.

Figure 2: Doppler Wind Measurement Spectral Response.

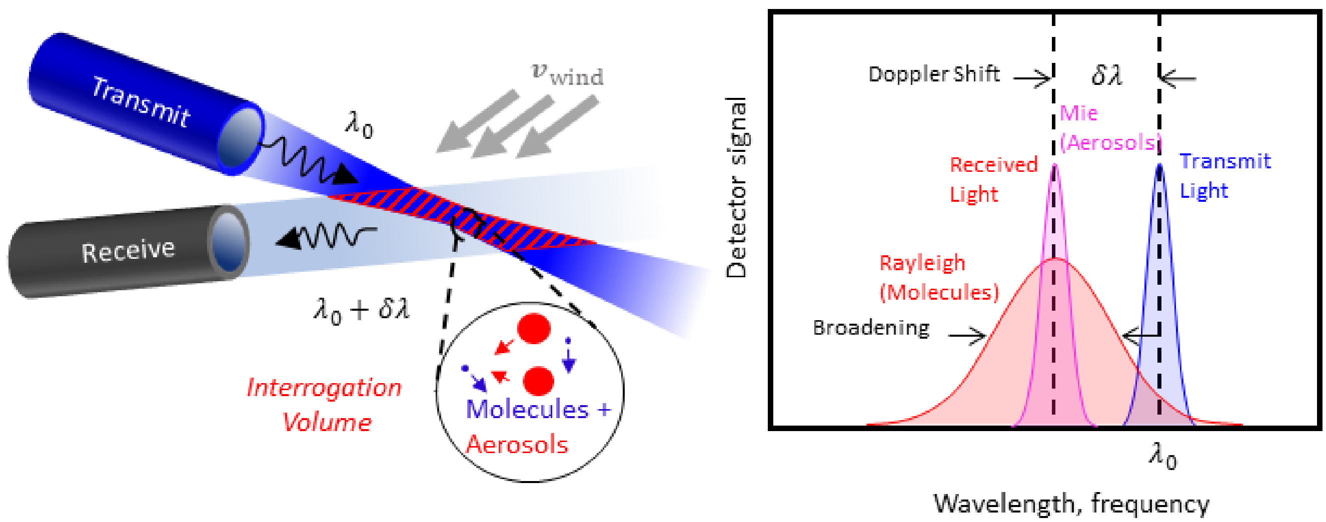

2.2.3. Doppler Scattering

Light scattering from a moving target undergoes a doppler shift. The wavelength shift of the light is related to the speed of the velocity of the scatterers relative to the speed of light. This manifests in the scattering wavelength from two different movements: 1) bulk movement of the atmosphere from wind and 2) random movement from thermal motion at the atmospheric temperature. Importantly, the ability to discriminate the amount of doppler shift from the two components allows the determination of atmospheric wind and temperature, respectively.

While all types of light scattering undergo doppler shifts, the higher signal levels of elastically scattered light provide a more practical route to determine atmospheric properties. The degree to which Mie scattering and Rayleigh scattering contribute, however, relates to the size of the contributing scatterers. The aerosols contributing to Mie scattering are large and heavy thus their thermal motion is quite small, manifesting in a negligible change in the linewidth of the outgoing laser. The molecules contributing to Rayleigh scattering, however, are quite small and light so their thermal motion is substantial (moving up to 500 m/s) producing a significant broadening of the linewidths, as shown in Figure 2. Both Mie and Rayleigh scattering show the bulk wavelength shift corresponding to the wind speed. This results in both Mie and Rayleigh scattering data contributing to wind speed calculations and only Rayleigh scattering contributing to a calculation of a temperature.

Importantly, these doppler shifts only detect movements along the line of sight of the telescope. Thus, a single measurement, with a telescope pointing along one direction in the atmosphere will only measure the wind component along that direction and cannot measure the full wind vector. Multiple telescope-pointing directions must be combined to solve for the unique wind vector.

2.2.4. Raman Scattering

The two types of inelastic scattering measured by HALAS, rotational Raman and vibrational Raman, are both based on the Raman effect. Named after the Indian physicist C.V. Raman, the scattered light has a different wavelength than the incident light. The wavelength difference relates to energy being transferred to/from molecular scatterers. Specifically, if energy is transferred to the molecule, then the light energy is reduced and becomes red-shifted (longer wavelength) called a Stokes shift. Alternatively, if energy is transferred from the molecule, then the light energy is increased and becomes blue-shifted (shorter wavelength) called an Anti-Stokes shift.

The amount of wavelength shift corresponds to the amount of energy taken/received from the molecular scatterer. Importantly, because the underlying mechanics are quantum mechanical in nature, these energy transfers come from energy level transitions leading to Raman lines with distinct wavelengths. Rotational and vibrational Raman scatterings have different energy levels. Rotational Raman constitutes the energy differences between quantum rotational states (how fast molecules are spinning) which is dependent on the rotational inertia of a molecule (weight and bond length). Vibrational Raman represents the energy difference between quantum vibrational states (how fast molecules are vibrating) which depends upon the bond strength of the molecule. Rotational energies are much lower than vibrational energy, with rotational Raman occurring between 0.1-3 nm away from the original wavelength of 355 nm. Importantly, because of the low rotational energy both Stokes and Anti-Stokes Raman scattering lines appear. Vibrational energies are much higher, with vibrational Raman occurring between 20-70 nm away from the original wavelength of 355 nm. Due to this higher vibrational energy, only Stokes Raman scattering lines appear. The expected spectra of both rotational and vibrational Raman scattering in the atmosphere are shown in Figure 3.

Figure 3: Spectral Profile of the Atmospheric LiDAR Scattering.

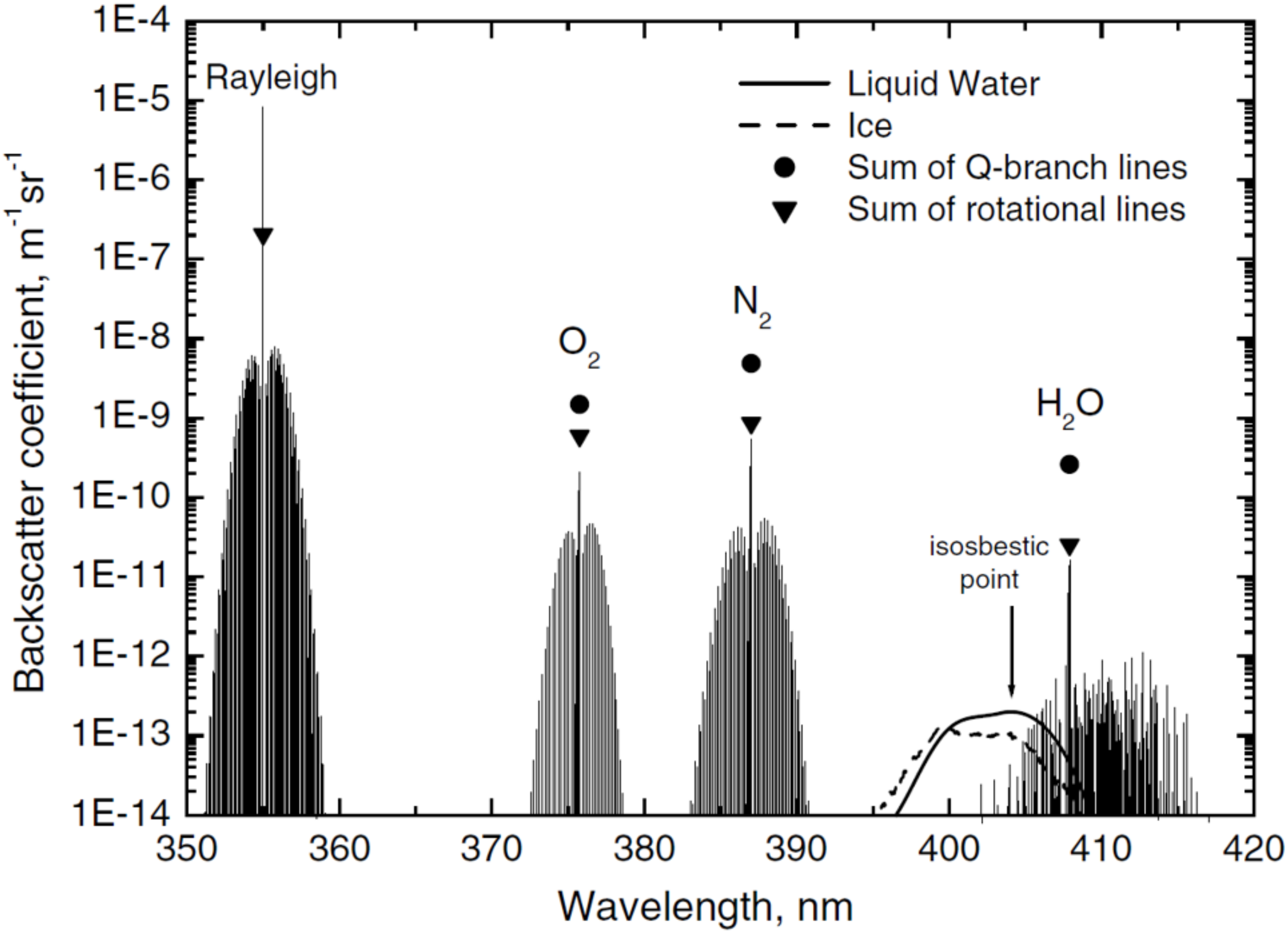

Another important feature in Figure 3 is the relative weakness of Raman scattering. It is several orders of magnitude weaker than Rayleigh scattering, which is in turn weaker than Mie scattering in certain atmospheric conditions, and usually has a spectral spread to the Raman lines as opposed to a singular distinct line as is the case for both Rayleigh and Mie scattering. Both qualities have consequences to signal to noise levels in a HALAS instrument.

2.2.5. Rotational Raman Scattering

Rotational Raman scattering directly probes the rotational energies of the main constituents of the atmosphere, nitrogen and oxygen. These diatomic molecules act as spinning rotors. The amount that the molecules are spinning is related to the thermal energy of the atmosphere. A higher temperature leads to a distribution of higher rotational energies while a lower temperature leads to distribution of lower rotational energies. The rotational Raman scattering directly probes these distributions due to the specific allowed optical transitions between different rotational energy states. The temperature difference in the expected nitrogen rotational Raman scattering response is seen in Figure 4. A lower temperature yields more intensity in wavelengths closer to the original laser wavelength of 355 nm, while a higher temperature increases intensity in wavelengths further from the original laser wavelength. By determining the intensity and spectral distribution of the rotational Raman scattering, the atmospheric temperature can be determined. Notably the rotational Raman spectra become more complex when both nitrogen and oxygen contributions are present as depicted in Figure 4.

Figure 4: Rotational Raman Spectra

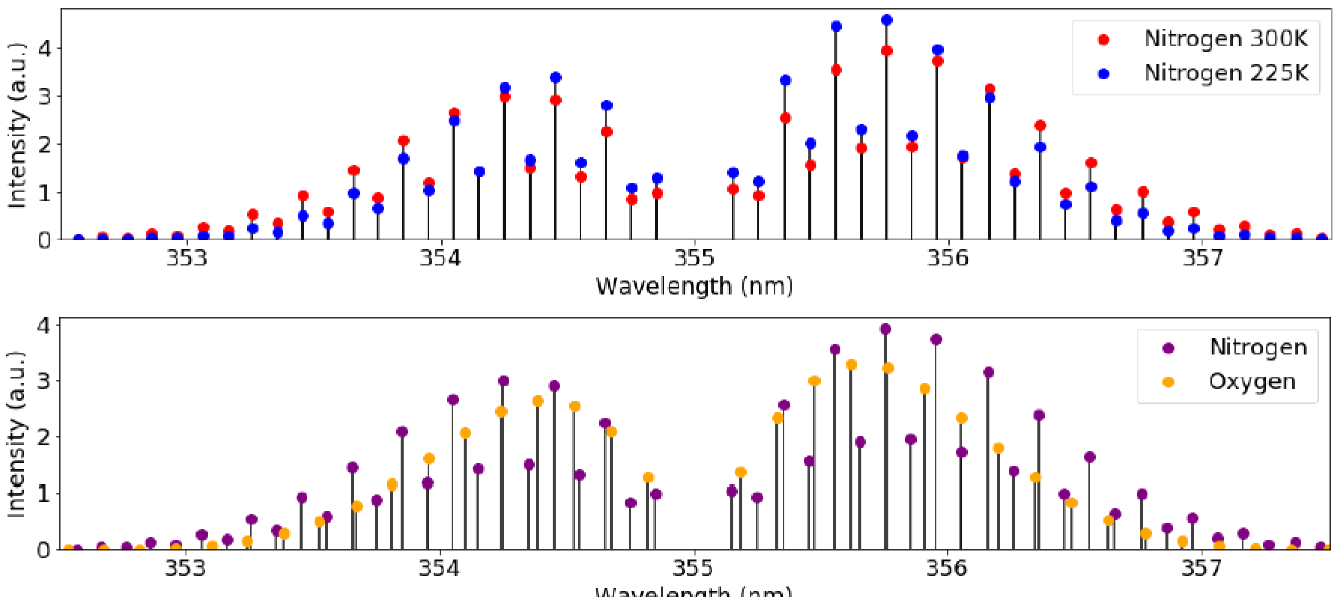

2.2.6. Vibrational Raman Scattering

Vibrational Raman scattering interacts with molecules, causing changes in their vibrational energy levels. Each atmospheric component has a unique vibrational energy structure which manifests as a unique vibrational Raman scattering wavelength. Specifically, the three main atmospheric components: oxygen, nitrogen, and water, all have spectrally isolated vibrational Raman features occurring at 376.8 nm, 386.7 nm, and 407.5 nm respectively seen in Figure 3. By filtering out each of these spectral features individually the quantity of each molecule in the atmosphere is directly related to intensity. Importantly, by measuring the water vapor vibrational Raman line intensity the water vapor content in the atmosphere can be directly calculated providing key insight into the atmospheric humidity.

2.3. LiDAR Equation

For several atmospheric data products, a spectral component of the scattering component is critical to the measurement, including the doppler shift and the spread of the rotational Raman signal. For other data products, however, most of the information is carried in the magnitude of the scattering signal. The intensity of a typical HALAS atmospheric return as a function of range (r) is determined by the LIDAR equation where C_0 is a constant to account for specific instrumental characteristics (laser power, telescope size…), $O(r)$ is the overlap function or the range-dependent collection efficiency due to telescope geometry, $\beta\pi(r)$ is the range-dependent backscatter cross-section, and $\alpha\lambda(r)$ is the range-dependent extinction cross-section at a wavelength of λ.

$$P(r) = \underbrace{\frac{C_0 O(r)}{r^2}}_{\text{I}} \underbrace{\beta_\pi(r)}_{\text{II}} \underbrace{\exp\left(-\int_{r_0}^{r} \alpha_{\lambda_{Laser}}(r')\,dr'\right)}_{\text{III}} \underbrace{\exp\left(-\int_{r}^{r_0} \alpha_{\lambda_{scat}}(r')\,dr'\right)}_{\text{IV}} \qquad \text{(Eq. 1)}$$

Equation 1 can be broken up into instrument/geometrical components color coded in Ⅰ, important atmospheric scattering components in Ⅱ, laser attenuation to the target range in Ⅲ, and scattering attenuation from the target to the telescope in Ⅳ. The instrumental and geometric considerations (Ⅰ) typically are important for understanding aspects of the instrument but do not contribute to atmospheric property calculations. The value of $\beta\pi(r)$ (Ⅱ) holds the most atmospheric information, as it relates to the quantity of the scatterer. For example, in Rayleigh scattering the air density is proportional to $\beta\pi(r)$ while in vibrational Raman scattering the water vapor content and humidity, nitrogen, or oxygen are proportional to $\beta\pi(r)$. The magnitude of the attenuation, both outgoing (Ⅲ) and returning (Ⅳ), also provide valuable information about the scattering quantities. It is important to note that for elastic scattering $\lambda Laser$=$\lambda scat$, which makes the outgoing and returning attenuation the same, while in Raman scattering these terms are subtly different.

An important distinction between elastic and Raman scattering is the contributors to of $\beta\pi(r)$ and $\alpha\lambda(r)$. For elastic scattering, aerosols contribute to the measured scattering and to the attenuation. For Raman scattering, however, aerosols only contribute to the attenuation. This makes Raman scattering less susceptible to aerosol contamination of the signal, shown in the equations below.

This allows for the identification of aerosol components and for flexibility in some atmospheric data product calculations that might otherwise be contaminated by the presence of aerosols.

$$\beta_\pi = \begin{cases} \beta_{\pi,mol} + \beta_{\pi,aero} & if\ elastic \\ \beta_{\pi,mol} & if\ Raman \end{cases} \qquad \text{(Eq. 2)}$$

$$\alpha_\lambda = \alpha_{\lambda,mol} + \alpha_{\lambda,aero} \qquad \text{(Eq. 3)}$$

For evenly mixed atmospheric components (ex. Nitrogen, Oxygen) the density decreases exponentially with altitude, decreasing by approximately 50% every 7.2 km (if the atmosphere is at a constant temperature). Correspondingly $\beta\pi(r)$ decreases in a similar fashion. Likewise, the geometric term (blue) of the LiDAR equation shows a quadratic decrease in signal with range. Together this means that the signal drops off dramatically with altitude. This is a challenge for atmospheric LiDAR measurements as the signal can often vary over many orders of magnitude necessitating detectors with a very high dynamic range spanning over 6 orders of magnitude, measuring from single photons to millions of photons. This has important implications on the detectors used for these measurements Figure 5 below depicts examples of P(r) as governed by Eq. 1 in real atmosphere from a ground HALAS system.

Figure 5: Example LiDAR molecular (left) and elastic (right) returns from HALAS system.

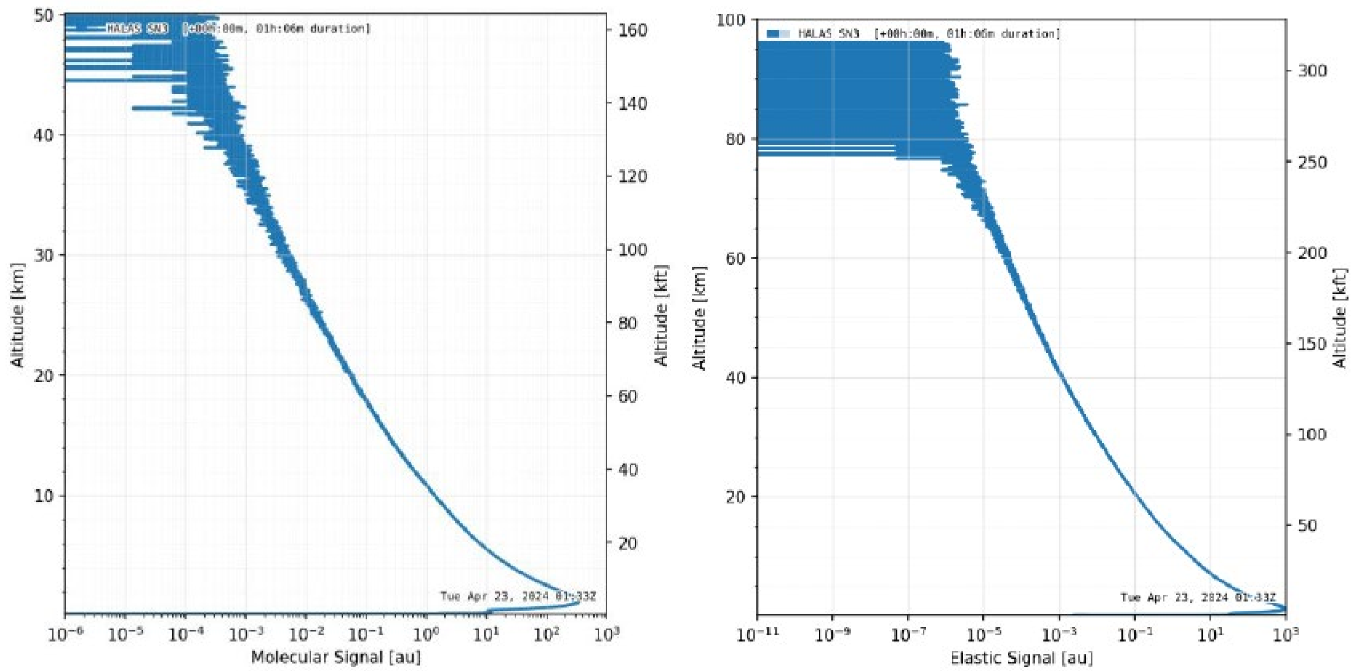

2.4. HALAS Core Components

Honeywell's HALAS system consists of the following main components:

- laser – to generate the optical pulses for LiDAR
- telescope – to collect the atmospherically scattered light
- science equipment – to examine and measure the scattered light for different spectral properties
- computer – to control instrumentation and process optical data into atmospheric data products

These core components represent the backbone of the LiDAR technology to turn a laser system into a weather instrument. While many additional components are necessary to practically make the system perform optimally, these are the core components that are common to every HALAS system.

2.5. Laser

HALAS laser systems have a few requirements to obtain high-quality atmospheric data.

1. Wavelength output at 355 nm

2. High pulse-energy output (up to 1 J/pulse)

3. Narrow linewidth emission

As mentioned previously, a UV laser system was chosen for the increased Rayleigh scattering efficiencies at lower wavelengths. At 355 nm, this is close to an ideal wavelength for atmospheric LiDAR as wavelengths below this are readily absorbed by ozone in the atmosphere and wavelengths above this value scatter less and have signals that suffer with competition from increased solar background. Further, 355 nm is a relatively common laser wavelength available from laser manufacturers. The 355 nm output is generated from a Nd:YAG (Neodymium-doped yttrium aluminum garnet) crystal. The Nd:YAG crystal emits at 1064 nm, is frequency doubled to 532 nm, and finally frequency tripled to 355 nm.

The need for a high pulse-energy laser is necessitated by the low scattering efficiency by Rayleigh and Raman scattering processes. Increased signal strengths help raise scattering signals out of any noise floors that exist including solar, detector, or others. Additionally, this improves the range of atmospheric measurement. This is usually done with a laser technique called Q-switching, where all the energy stored in a laser cavity is released in a single laser pulse. This is further aided by sending the laser pulse through additional Nd:YAG amplification stages.

Making highly performant wind measurements requires an accurate measurement of the doppler shift. This is made possible with a low-linewidth laser. In this way small doppler shifts are easily measured as the wavelength shifts a substantial fraction of the linewidth. This is enabled by seeding the Nd:YAG laser with a stable, low-power, narrow linewidth laser (called a seed laser) to stimulate emission from the higher power laser at the same wavelength of the seed laser.

2.6. Telescope

HALAS systems incorporate a telescope to capture the backscattered atmospheric scattering. To enable this collection the telescope field of view must be coaligned with the outgoing laser. It focuses the returned light onto an optical fiber to send the scattered signal to the science equipment.

The telescope, however, captures light scattered from any object in the telescope field of view. This includes solar light scattered by atmospheric constituents or hard targets. To minimize the amount of background signal collected by the field of view of the telescope must be minimized. This is done by focusing the telescope to infinity which collimates the field of view meaning that the diameter of the field of view is <10 m even 10 km away from the telescope.

Similar to the laser, the telescope has a high impact on the signal levels of the collected atmospheric scattered light. The signal ratio is proportional to the area of the telescope or proportional to the square of the diameter making this a critical parameter for performance. This leads to the need for large telescope diameters, with 14” and 24” diameter telescopes in current HALAS systems.

2.7. Science Equipment

The optical interrogation of the different atmospheric scattering signals is performed by multiple instruments and detectors. These four instruments are: the Interferometer, Spectrograph, Rayleigh Recycle Box, and Sky Filter Box. The different types of scattering are spectrally filtered and sent to individual instruments designed to examine a specific atmospheric property seen in Table 1. This filtering is performed in the Sky filter box using thin-film interference dielectric mirrors.

Table 1: HALAS detection channels and descriptions

Channel	Description
Interferometer	High-resolution interferometer detecting spectral broadening and Doppler shifts in the Rayleigh and Mie returns
Rayleigh Recycle	Sensors detecting the Rayleigh and Mie return
Spectrograph	A spectrometer detecting the rotational Raman return
Sky Filter Box	Sensors detecting the N_2 and H_2O vibrational Raman return

The Rayleigh and Mie scattering initially are sent to the Interferometer which measures the doppler shift using a high resolution Fabry–Pérot interferometer to determine the atmospheric wind speed. The Rayleigh and Mie scattering that is reflected by the Fabry-Perot interferometer is recollected and sent to a separate detector called the Rayleigh Recycle Box to determine the high-altitude density. The rotational Raman signal is sent to the Spectrograph which measures the spectral spread and intensity of the rotational Raman scattering return to determine atmospheric temperature. Lastly the water and nitrogen vibrational Raman signals are kept inside in the Sky Filter Box, spectrally separated by more dielectric mirrors, and measured individually.

Crucially, this science equipment is common to all HALAS systems which allows for robust operation of these instruments by extensive testing. This also improves data analysis capabilities as algorithms are fine-tuned for the common set of instruments. Further these technologies can benefit from both software and hardware improvements as Honeywell continually works to improve both.

Figure 6: Spectral Separation and Measurement of Atmospheric Scattering Light with the Science Equipment.

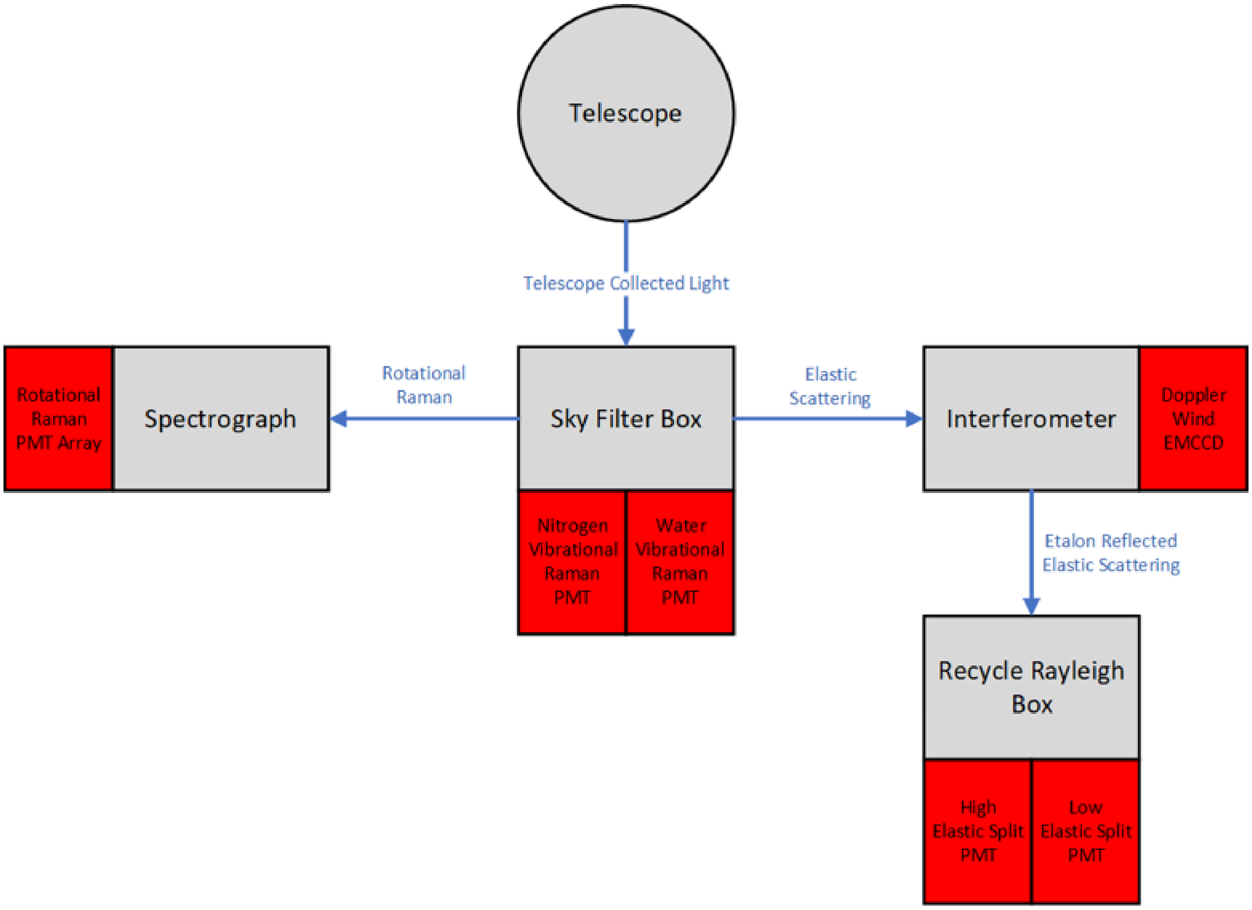

2.7.1. Sky Filter Box

The Sky Filter Box has two main tasks: 1) spectrally separate the various scattering signals captured by the telescope and 2) measure the vibrational Raman scattering signals from the nitrogen and water channels.

The scattering signal separation is accomplished by using a series of filters described in Figure 6. First the vibrational Raman channels are split from the elastic and rotational Raman features. This is accomplished using a dichroic filter with a split around 360 nm. The elastic and the rotational Raman signals are separated using a narrow linewidth bandpass filter around 355 nm, which passes the elastic signal and reflects the rotational Raman signal. The vibrational Raman signals are further split into the nitrogen and water vibrational Raman channels with a dichroic filter with a split around 400 nm. Like the telescope signal, the output of the rotational Raman and elastic signals are fiber coupled to enable simple transport of signals to additional science equipment.

The measurement of the vibrational signals is done simply once the signals are split. Each of the nitrogen and water channels is measured using photomultiplier tubes (PMTs). Before each of these measurements, however, a narrowband filter is used to exclude signals outside a small spectral region around the vibrational Raman signal 386.7 nm and 407.5 nm respectively for nitrogen and water. This is done to exclude the solar background. This is particularly important for daytime operations or in environments with significant ambient light. During these daytime operations, the solar background light is in the full spectrum. It is crucial to remove the light that is outside the wavelength bands useful for determining atmospheric parameters. Thus, effectively removing light of different wavelengths is critical for improving the system's signal to noise ratio (SNR).

2.7.2. Interferometer

The interferometer has the main task of measuring the doppler shift of the Mie and Rayleigh scattered light. This is done by using a specialized interference technique to accurately measure the altitude-dependent doppler shift.

An interferometer works by measuring the phase shifts in optical signals. These phase shifts are used to measure the small wavelength shifts associated with the doppler shift which manifest as phase shifts in the interferometer. The high-resolution phase measurement requires the use of a high-finesse interferometric technique, with a Fabry–Pérot interferometer chosen for this application. A Fabry–Pérot consists of two parallel, highly reflective mirrors called an etalon. When light enters the etalon, it bounces back and forth between these mirrors, creating multiple reflections. This setup causes the light waves to interfere with each other, creating constructive and destructive interference patterns. By analyzing this interference pattern, a precise measurement of the phase shift associated with the doppler shift is made.

A Fabry–Pérot interferometer, however, generates a circular interference pattern when imaging the light exiting the optical fiber. This becomes problematic when attempting to measure the doppler shift at different altitudes. Each altitude would require a readout of the entire 2-dimensional circular interference pattern, requiring a camera to collect an entire image in the timescale of ~100 ns. Detectors are unable to perform at this level while also measuring extremely small amounts of signal. This issue is resolved using a non-spherical optic called a CLIO. This atypical optic transforms the circular fringes into 1-dimensional (1-D) linear fringes. This allows the use of a fast 1-D detector or a 2-D camera that is streaked to turn one of the camera dimensions to be used into a time axis in a technique called streaking. Specifically, the instrument uses a streaked EMCCD camera to analyze the optical signal. This allows for the doppler phase shift to be measured at many altitudes enabling a measurement of an atmospheric wind profile.

2.7.3. Spectrograph

The spectrograph has the main task of measuring the rotational Raman spectrum. This is done by using common spectral dispersion techniques with a diffraction grating.

A spectrograph measures the wavelength dependence of the optical intensity profile. Specifically, the light falls on the dispersive element, a diffraction grating in this case, which maps a wavelength distribution onto an angular distribution. After focusing, this distribution becomes a position distribution. This allows the wavelength distribution to be measured on a linear detector which each detector pixel measures a different wavelength. Due to the low signal levels and fast readout time a 32-PMT array was chosen to examine the rotational Raman spectra. This spectrally resolved rotational Raman signal can be used to measure the atmospheric temperature.

2.7.4. Rayleigh Recycle Box

The Rayleigh Recycle Box has the main task of measuring the elastic signal that is recovered from the Interferometer. The etalon in the interferometer is a highly reflective surface that transmits only ~30% of the light for interferometric analysis. The remaining 70% of light is reflected off the surface of the etalon, collected and sent to the Rayleigh Recycle Box to be measured with a higher dynamic range detector than an EMCCD camera. Specifically, the signal is measured with a PMT, although even the PMT is unable to capture the full dynamic range of the atmospheric signal (~1010 change of signal between low and high altitudes) and several PMTs are strung together each capturing a different intensity region of the atmospheric signal and combined in a post-processing capacity to generate an even larger dynamic signal measurement.

2.7.5. Detector Capabilities

The current optical detectors are a combination of PMTs and EMCCD cameras. Each of these detectors have different operating capabilities and features that make them useful for different operating conditions. Both types of detectors, PMTs and EMCCDs use an electron multiplication method to lift the low light signal out of other noise sources to make highly robust measurements under low light conditions. The ability to make these low-level light measurements is crucial for HALAS technology where weak atmospheric scattering often makes signal photons scarce especially at high altitudes.

PMT detectors have the following characteristics:

- Single-photon detection capable
- Very high dynamic range with transient recorder data capture (currently only capable for single-element detectors)
- Limiting thermal noise for analog detection, but does not limit single-photon detection
- Multi-element array possible, limited to small linear arrays
- High-speed detection

PMTs convert photons into electrons using a photocathode. These ejected photoelectrons then get multiplied by a series of high-voltage dynodes which serve to multiply the ejected electron. In this way a single incident photon causes a cascade of many electrons detected on the detector anode. This process turns input light signals into electrical signals and readily measured with data acquisition systems. Specifically, the PMT current can be directly measured with an analog to digital (A2D) converter. However, the PMT measures the noise as well as the desired photocurrent. This prevents robust measurements at low photon counts. PMT currents can also be analyzed to count individual photons. This is done by counting current spikes which correspond to the cascade of photo electrons. Taken together, PMTs can allow for simultaneous photon counting measurements and analog measurements of the photocurrent. This simultaneous measurement through a device called a transient recorder, enables high dynamic measurements of optical signals making it a crucial detector for HALAS measurements.

EMCCD cameras have the following characteristics:

- Single-photon capable, however, seriously limits dynamic range
- Moderate dynamic range
- Low thermal noise (chilled detector), but limiting read noise (low gain settings)
- Large arrays readily available
- Slower detector response

EMCCDs are detectors that use a normal CCD architecture where photons are converted into electrons in a photo-active layer in the device. These electrons are captured in a potential well and accumulated during the exposure of the image. Then they are shuffled sequentially and measured one by one. In an EMCCD detector the captured electrons are multiplied in a series of electron multiplication stages. This is important as it lifts the signal above the read-noise of the detector.

`While the electron multiplying gain can be set high enough for single photon counting, this is not typically done as it has serious limitations in the maximum photon collection rate. Instead, lower electron-multiplying gains are used to maximize the dynamic range, which is limited by the noise floor of the detector, and to maximize the electrons that can be captured in the potential well.

2.8. Analysis Computer

The detector signals measured above are read into the analysis computer. Importantly, while the mapping between detector to atmospheric data product may seem straightforward, often it is necessary to use multiple detector signals as aiding values to improve the robustness and reliability of the measurement as shown in Table 2.

Table 2: Relationship between sensor measurements and derived data products

Sensors \ Data Products	Air Density	Wind Vector	Temperature	Humidity
Fabry Perot Interferometer	Aiding	Required		
Elastic Scattering	Required	Aiding		
Rotational Raman Scattering			Required	Aiding
Vibrational Raman Scattering	Required			Required

Legend: Required (green) Aiding (blue)

3. HALAS Systems

HALAS systems must have a considerable number of ancillary subsystems, infrastructure, and software to meet all the operational needs of the instruments. The specific configuration of the supporting equipment depends upon the HALAS system with drastically different needs for airborne and ground systems. The general subsystems can be broken down into the following groupings: Transceiver, Core Sensor, Software and Algorithms, and Infrastructure seen in Figure 7 below.

Figure 7: General HALAS System Architecture

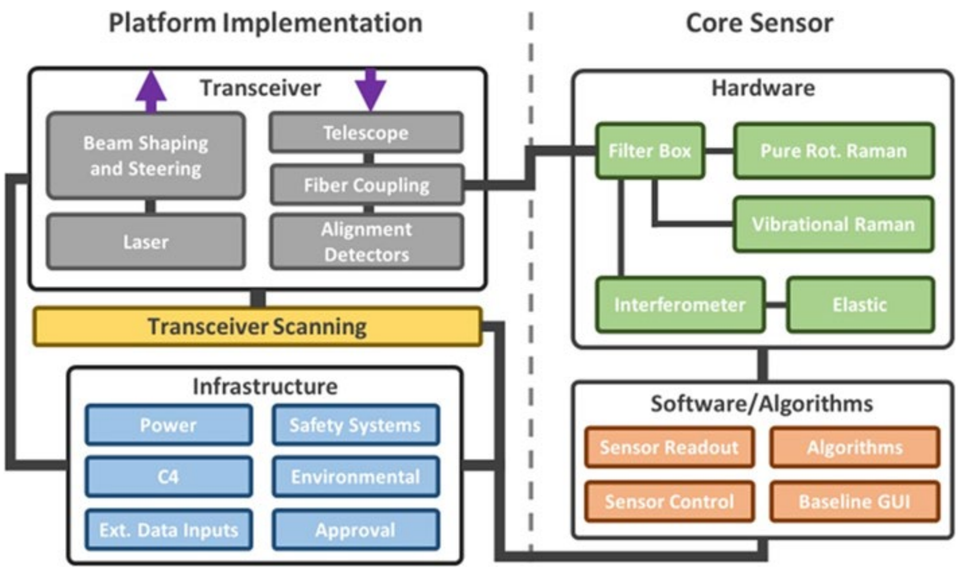

3.1. HALAS System Historical Overview:

HALAS technology comprises multiple measurement platforms including both ground-based HALAS units and airborne HALAS units. The HALAS ground systems are fixed stations that can be transported between locations of interest to make atmospheric measurements. These ground systems are mature systems with initial prototypes deployed since 2014, with upgraded units in deployment since 2020, and four units currently in deployment. The HALAS airborne systems are aircraft integrated systems that are mobile and can make measurements on location and on-demand. A prototype instrument was integrated on a Gulfstream aircraft between 2020 and 2022. The development of an instrument to be installed onto an unmanned aircraft is ongoing with initial test flights occurring in Q4 2024.

HALAS ground systems have been extensively field tested from Kwajalein (Marshall Islands), Edwards AFB (CA), Vandenberg SFB (CA), Pt. Mugu NAS (CA), Cape Canaveral (FL), White Sands Missile Range (NM), Spaceport America (NM), Wallops Flight Facility (VA), Sterling Field Support Center (VA), Honeywell's Plymouth facility (MN), a collaborator's facility (MI), and a private space-launch facility (TX). Substantial system improvements have been made since 2019 with improved performance, reliability, operational capabilities, and automation.

HALAS Gulfstream system logged more than 200 hours of measurements during flights at locations throughout the Pacific Ocean, California, and the Midwest United States. The 2nd generation of HALAS Airborne System has begun flight tests from Edwards Air Force Base (CA).

3.2. HALAS Ground System Overview

The HALAS ground system is a ground-operated atmospheric unit shown in Figure 8. The units are housed in a modified shipping container and contain all the core HALAS components described previously but many ancillary components that provide reliable and safe operation, easy transport, maintenance, and operator accommodations. To include all these necessary features the HALAS ground system currently has a substantial size, weight, and power (SWaP). It weighs 23,000 pounds, occupies 20' x 8' x 12' volume (stowed), and requires up to 10 kilowatts power.

Figure 8: HALAS ground system picture at Sterling Support Center in Virginia.

3.2.1. Transmit and Receive Module (TREX)

The transmit and receive module (TREX) includes the components needed to transmit the laser into the atmosphere including: the laser and the beam shaping/steering hardware, as well as the components needed to receive the scattered light including: the telescope, fiber coupling, and alignment detector. For the ground system, the TREX contains all the necessary components to drive the operation of both the transmit and receive modules. Importantly, keeping the transmit and receive paths contained in a single mechanically rigid unit maintains coalignment between the transmit (laser) and receive (telescope) paths in a robust fashion.

The TREX module houses the high-power laser, capable of generating laser pulses up to 1 J/pulse at a repetition rate of 10 Hz. It also contains the 24” telescope. Together this combination of high-power laser and relatively large telescope allows for sufficient backscatter collection that enables high altitude measurements from ground level.

3.2.2. TREX Scanner

The TREX is mounted onto a motorized platform that can rotate 0-360° azimuthally and 0-90° in elevation. This allows the TREX module to scan anywhere in the full hemisphere. This scanning mobility is crucial for multiple pointing directions needed for a full wind vector measurement. The robust coalignment of the transmit and receive modules allows for this scanner to quickly change pointing directions as needed for the measurement.

3.2.3. Bean Shaping and Steering Optics

Control and manipulation of the output laser is critical for appropriate atmospheric scattering and safe/reliable operation of the HALAS instrument.

Coalignment between the telescope and outgoing laser is crucial for appropriate collection of the scattered light. If they are not coaligned the light scattered from the laser will not be inside the field of view of the telescope and will not be collected. To align the transmit and receive paths it is simpler to steer the laser than orient the telescope. This is accomplished by two actuated mirrors directing motion in semi-orthogonal axes. In this way the laser can maintain alignment with the telescope even under conditions when there is a mechanical drift between the transmit and receive paths.

Another important manipulation of the laser beam is the expansion of the beam diameter. This 10x beam expansion has two important implications: 1) a larger beam diameter reduces the divergence of the laser with range helping maintain a smaller beam diameter at long range and 2) a larger beam diameter reduces the intensity of the beam providing safer operation of the laser by reducing the hazard both to personnel and optical components in the beam path.

Other beam manipulations and characterization devices are installed in the path of the laser prior to transmit. A small amount of laser light is split and sent to the interferometer as a source of the reference wavelength of the original laser light prior to a doppler shift.

3.2.4. Fiber Coupling

Fiber coupling involves directing the collected scattered light from the telescope into an optical fiber, which then guides the light to the detectors. Optical fibers are used to transmit the collected light with minimal loss and to allow flexible routing of the light to the detector. This allows the detector and TREX module to be in separate locations enabling the TREX module to be scanned without consideration of the optical alignment of the science equipment. Further, this fiber coupled setup helps isolate the detector from environmental vibrations and movements.

3.2.5. Alignment Detectors

In addition to the main optical signal fiber where most of the atmospheric scattering signal is collected and distributed to the science equipment, there are additional alignment fibers that surround the main fiber. The purpose of these fibers is to determine if the laser is aligned with telescope. These fibers send signals to PMT detectors. The general use case of these alignment fibers is to detect if the atmospheric scattering light is collected by these alignment fibers instead of the main fiber. In this way the laser beam can be steered using the beam steering optics to direct the scattered light towards the main signal fiber.

3.2.6. Core Sensors

With the telescope collecting the scattered signal, the light is transmitted through an optical fiber, which then guides the light to the science equipment. This science equipment is core to all HALAS systems including the HALAS ground system and was described in Section 2.7.

3.2.7. Safety System

The use of a high-power laser necessitates appropriate safety measures to be in place to ensure safe operation of that laser. This includes range safety (safe operation in compliance with an operational location, e.g., air force base, airport, etc.), Laser Clearing House (LCH, safe operation with respect to satellite assets), and Federal Aviation Administration (safe operation in compliance with commercial aircraft).

Control of the high-power laser is done with both a low-power shutter interior to the laser and a high-power shutter exterior to the laser. Under typical operational conditions, the high-power shutter is used to prevent the emission of the laser from the TREX module. This is done in part automatically in compliance with the LCH guidelines and with tracking of commercial aircraft via Automatic Dependent Surveillance–Broadcast (ADS-B). In addition, a human spotter is used to ensure laser safety onsite. The low-power internal shutter offers a redundant mechanism to allow the ability to prevent laser emission in the case of failure. Additionally, mechanisms are put in place that prevent laser emission in the case of software crashes and connectivity problems of a remote operator.

3.2.8. Control Software

The operation of such a complex instrument requires a considerable amount of software automation. This includes the movement of the TREX, alignment of the steering mirrors, operation of the laser, initiating and collecting data from the core science equipment, and laser safety. Many of these features operate without substantial operator intervention, with the operator required to set up an atmospheric data collection corresponding to the data needs and to monitor laser safety. This operator interfaces with the instrument through a graphical user interface (GUI) that can be accessed remotely.

The GUI affords many additional capabilities to the user. The GUI provides direct monitoring and control of each hardware component. It also allows the operator to terminate or pause the operation when weather conditions change, nearby aircraft are present, or a particular hardware device failure occurs. The operator can also monitor the science equipment data in real time to ensure acceptable detector performance and quality checks of the atmospheric scattering signal.

3.2.9. Data Storage and Analysis Infrastructure

For each HALAS ground system, the science instruments collect data for the outgoing laser pulse, with some doing so on a per pulse basis. This represents an exceptionally large amount of data collected. Thus, a server with optimized data storage and data processing capability is crucial to ensure quick data analytics to be completed immediately after each operation. Due to the volume of the data collected, the data must be analyzed locally. The data analysis is done automatically with remote access to the analysis server to ensure smooth analysis and quality control of the final atmospheric data products. The software then generates plots and reports based on the format requested by the customer.

3.2.10. Infrastructure and Accessories

To ensure the entire HALAS system operates effectively, several additional hardware components and accessories are required. These include:

1. **Power Supply:** All the hardware requires a reliable power supply. Part of the infrastructure must provide power to each piece of equipment and maintain temperature control for the laser, TREX, camera, etc. The entire system has power consumption exceeding 10 kW during operation, which is higher than the usage of a single-family house. This power is currently provided by grid hook-up at the customer facility. In the new generation, the ground-based HALAS will have significantly reduced power consumption. In the airborne-based system, power consumption has already been significantly reduced as detailed in Section 5. To ensure safe and reliable operation, the battery backup or alternative power supply could be utilized to ensure continuous operation under various conditions, even when the grid power is not available.

2. **TREX Lift Stack:** The TREX on the HALAS ground system is designed to be stowed inside the instrument when the instrument is not performing measurements, during inclement weather, maintenance, and transport. This TREX stack allows for quick deployment of the HALAS system, so it is ready to collect atmospheric data within minutes. Additionally, this setup is robust for instrument transport by safely stowing the sensitive optical equipment during travel. This also allows for rapid deployment of an entire HALAS ground system within a few days.

3. **HVACs and Temperature Control Systems:** Various heating, ventilation, and air-conditioning (HVAC) systems and chillers are necessary to maintain optimal environmental conditions for the laser, the TREX, and the overall HALAS system. The heating element is also built into the laser to ensure the initial warmup of the laser for operation. These systems also ensure the camera sensor remains at a low temperature to minimize electronic noise and maintain high SNR. Additionally, various sensors and sensor networks are installed to monitor the thermal conditions of each component and subsystem and the entire container. For example, temperature sensors are used to monitor each device's operational condition and fluid monitors are used for the liquid cooling systems of lasers and other devices.

4. **External Data Inputs:** External data sources are used to ensure safe and reliable HALAS operations. For example, security cameras are installed for safety operations and to monitor environmental conditions and nearby aircraft. Additionally, the system utilizes ADS-B data, which is broadcasted by all commercial aircraft to provide their position, velocity, and other relevant information. This data is used to determine if there are nearby aircraft that require the laser to be shut down, ensuring safe operation. Therefore, a proper network connection is required, and software for acquisition of these inputs has been developed and implemented in the HALAS system.

5. **Safety Protection, Security, and Emergency Response Setup:** Various safety measures and emergency response setups are in place, particularly for laser safety and severe weather responses. This includes protocols for power outages and ensuring that certain regions are restricted from human entry during Trex operation to maintain safety. Currently, even with cameras and ADSB monitoring for aircraft, a human spotter is required to be on-site to monitor for aircraft and use manual buttons to close the laser shutter when nearby aircraft enter HALAS LOS. The security cameras remotely monitor unauthorized personnel access and monitor weather conditions.

6. **Regulatory Compliance and Permits:** Maintenance of various approvals and permits as required by law and facility owners are essential. This includes compliance with regulations related to laser operation, environmental impact, and safety standards.

3.3. HALAS Airborne System Overview

3.3.1. 1st Generation Gulf Stream Description

The HALAS system was installed onto a Gulfstream IV aircraft. The Gulfstream HALAS system was operated from 2020 to 2022 with flights throughout the Pacific Ocean, California, and the Midwest United States. This system used a fixed, upward-facing telescope to perform atmospheric measurements including density, temperature, and wind vector measurements. To acquire the multiple lines-of-sight required for a doppler wind measurement of the wind vector, the system would follow circular flight paths around particular points of interest, directing the fixed telescope in a full 360° arc. With a typical flight altitude of >40,000 ft, this platform was able to operate independent of weather conditions by making clear-air measurements above the cloud layers. Crucially, this system acted as a testbed for further development of airborne platforms including the 2nd Generation of HALAS Airborne System.

3.3.2. 2nd Generation of HALAS Airborne System Description

An unmanned high altitude aircraft offers a highly advantageous airborne platform for HALAS measurements. The higher altitude ceiling of ~60,000 ft allows for atmospheric measurements higher in the atmosphere. The longer flight endurance of up to 24 hours allows for long-range missions, many measurement locations, or time-coarse measurements.

The 2nd Generation of HALAS Airborne System retains all the atmospheric measurement capabilities of the ground systems including temperature, density, humidity, and wind vector. Like the Gulfstream system, the 2nd Generation of HALAS Airborne System uses a fixed telescope. In order to retrieve a wind vector, the aircraft must perform flight maneuvers to achieve multiple lines of site.

Integration of the 2nd Generation of HALAS Airborne System into aircraft platform, however, required considerable advancement of the HALAS technology including ruggedization, SWaP optimization, and fully remote operation. Specifically, the finalized SWaP estimate of the system resulted in a 620-pound instrument which fits in 25 cubic feet space and draws a maximum power of 1000 watts.

3.3.2.1 Laser

The biggest trade from HALAS ground to the 2nd Generation of HALAS Airborne System is the use of a ruggedized laser system. Specifically, transitioning from a flash-lamp pumped system to a diode pumped Nd:YAG laser with space-based heritage. This yielded a low-maintenance, ruggedized, and SWAP-optimized system. The diodes have substantially longer lifetimes than flash-lamps eliminating the need for maintenance to replace these components. The diodes also provide much higher efficiency, yielding a 7 W UV output for only 300 W of wall power. Further the ruggedized and SWAP-optimized package has space-based legacy and resulted in an overall package that was 10× smaller volume and 4x lighter.

3.3.2.2. SWaP Optimization

In addition to the SWaP optimization of the laser, many other subsystems were miniaturized and ruggedized. The telescope was reduced in size to 14” (0.36 m) to ensure the size and weight were compatible with integration while maintaining enough signal for the atmospheric measurements. The science equipment was modified from using commercial-off-the-shelf (COTS) components to a custom miniaturized system. Not only did this yield a smaller and lighter system, but the performance of the atmospheric measurement devices was improved. A smaller onboard computer replaced the control server, and the analysis server was omitted limiting atmospheric data delivery to post-processing only and no live data. The timing subsystem, thermal subsystem, power distribution subsystem, and safety subsystem were all made smaller with both changes to COTS component selections and custom designed systems. Lastly, the solely remote operational nature of the 2nd Generation of HALAS Airborne System reduced the need for operator accommodations reducing size, weight, and power.

3.3.2.2 Ruggedization

Throughout this redesign process, numerous ruggedization improvements were made. The primary ruggedization effort focused on the laser, core science equipment, transmit optical components, and enclosure. The laser was in part chosen due to its known heritage in space-based applications well beyond the required ruggedization efforts for the high altitude aircraft. The redesigned science equipment was examined with finite element methodologies to ensure rugged fixturing and enclosures of the devices along with maintaining high performance under the expected operational conditions. The transmit optical component including the optical bench and telescope also underwent finite element methodologies to ensure rugged operation. The enclosure was optimized for lightweight and rugged operation.

3.3.2.4. Environmental Systems

The HALAS GH system resides in an environmentally uncontrolled portion of the aircraft. Therefore, the environmental control system of the HALAS GH maintains the temperature of the internal components of the HALAS sensor. This includes cooling both the air-cooled and liquid-cooled components. Critically, the laser is controlled to ±1 C of the target temperature to ensure optimal performance of the laser. The extracted heat from the system is dumped into the exterior airstream. Environmental control also supports multiple states that heat or cool the HALAS system to different extents to operate or conserve power.

4. Measurement Performance

The HALAS ground system offers continuous, near real-time atmospheric measurements from a ground-operated unit. A full altitude-resolved vertical profile is measured simultaneously with the detectors detailed above. Nominal operations of the HALAS ground system provide a suite of atmospheric data products including wind vector, humidity, density, temperature, and cloud height measurements.

These atmospheric measurements have a nominal data collection configuration of ~1 hr integration time and ~12 lines of sight spread evenly across approximately 360° in azimuth with an elevation angle of 60° seen in Figure 9. The data processing time, while under continuous improvement, is typically ~10-15 min with data curated based on uncertainty limits and known anomalous atmospheric conditions.

Figure 9: Image showing typical lines-of-site measured within a fixed cone by HALAS ground platform while deployed at Sterling Field Support Center

A detailed summary of typical operational performance and data characteristics for all data products is provided in Appendix 1. Table 3 provides a summary of the current ground system 3D wind measurement performance with respect to the requirements listed in Table 2 of Broad Agency Announcement on this topic. Due to the different design and application of the ground-based HALAS versus a proposed satellite-based HALAS, not all categories in the table are applicable to the ground-based variant (e.g., coverage area) and many performance characteristics are likely to change in the new space-based application of HALAS within a trade space as will be detailed in the Space Variant Report for Honeywell Atmospheric Winds Campaign for Space. Table 3 importantly demonstrates that the ground-based HALAS system is currently meeting most requirements and many of the maximum requirements for a space-based version so its data products, particularly wind, can serve as a sufficient stand-in for studies in how a space-based HALAS could benefit the weather enterprise if successfully meeting BAA Table 2 requirements.

Table 3: HALAS Ground System 3D Winds Performance and BAA-NOAA-3DWinds-2022 Requirements Met

Attribute	HALAS Ground System Performance	Requirements Met (Minimum, Mid-Point, Maximum, or N/A)	Notes
Minimum Coverage Area	1.5-23 km*	N/A	Coverage area depends on number and horizontal density of ground system. Regional is feasible; global is not due to oceans.
Update Rate	5*-60 minutes	Maximum	User-specified update rates down to 5 minutes are possible with a 60-minute running average
Latency	15 minutes	Maximum	
Horizontal Resolution	1.3-23 km*	Maximum	Horizontal resolution depends on the number and horizontal density of ground systems. Sacrificing horizontal resolution for coverage area is likely required in a ground network.
Vertical Resolution	130 m <12 km 260 m <32 km	Maximum	
Uncertainty: Direction	15° <10 km (at 10 m/s)* 30° <20 km (at 10 m/s)*	Minimum (<10 km)	Varies with wind speed

Attribute	HALAS Ground System Performance	Requirements Met (Minimum, Mid-Point, Maximum, or N/A)	Notes
Uncertainty: Speed	1-2 m/s <10 km 4-6 m/s <20 km	Maximum (<10 km) Mid-point (<20 km)	
Vertical Extent	1.3-20 km (lower troposphere to lower stratosphere)	Minimum*	Coverage extending 5-10 km above tropopause and into the lower troposphere (but not the surface layer) is possible which exceeds the Minimum requirement

4.1 Nominal Wind Measurement

Atmospheric doppler wind measurements that can be calculated by HALAS data include northerly and easterly wind vector components or wind speed and wind direction. A typical wind dataset taken at NOAA's Sterling Field Support Center is shown in Figure 10 where the HALAS measurement displays excellent agreement with radiosondes launched at the same time and location. The typical maximum altitude of wind measurements is ~20 km, the horizontal cone then has a maximum lateral extent of also ~20 km (see Figure 9) when measuring at that maximum altitude with a proportional decrease in measurement area with decreasing altitude. The resulting wind measurement has a typical altitude resolution of 130 m and 260 m below 10 km and below 20 km, respectively. This smaller resolution at lower altitudes is enabled by increased signal strengths at low altitudes allowing for the native detector resolution to be used (130 m) whereas higher altitudes have reduced signals necessitating larger altitude bins to increase photon counts and drive down wind uncertainty. The final wind vector components yield uncertainty of <1-2 m/s and <4-6 m/s for below 10 km and below 20 km, respectively. Importantly, wind measurements below 1.3 km are not possible due to the geometric constraints of the telescope and optimization for high-altitude data collection.

Figure 10: HALAS Example Wind Measurement.

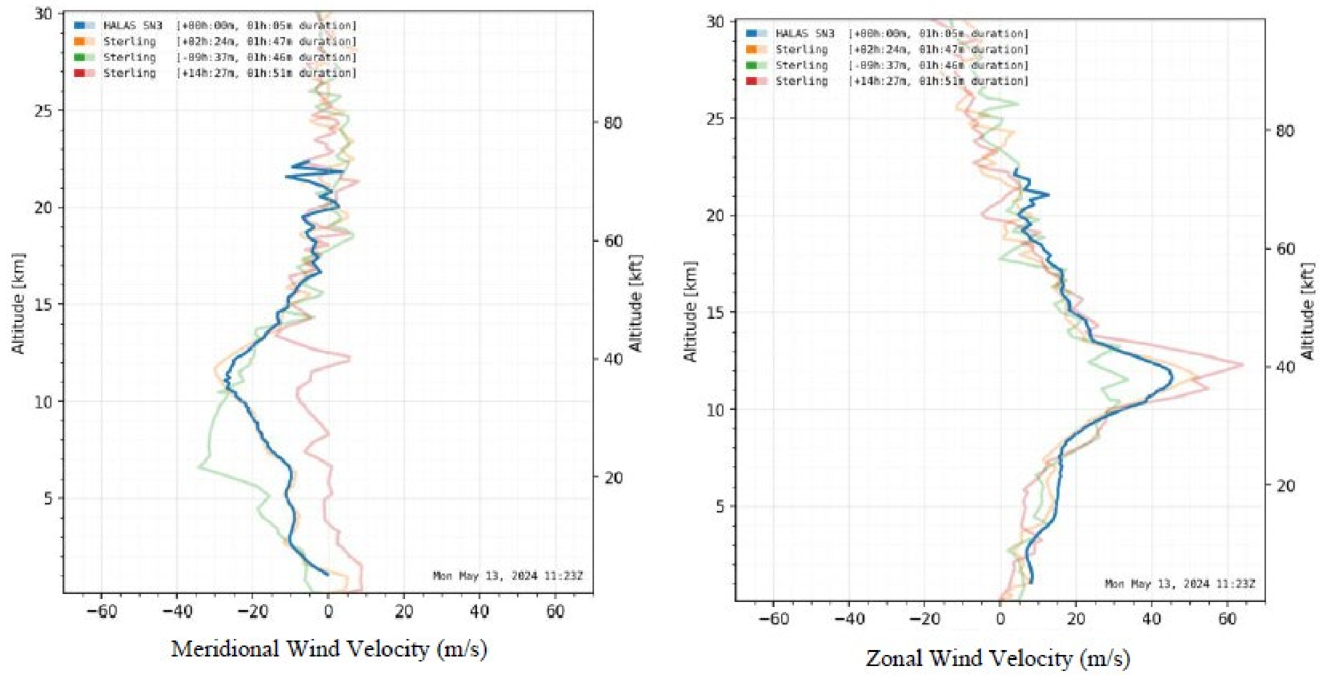

These measurements have been validated throughout many measurement campaigns, some of the most recent highlights include comparative studies to the 48 MHz Tropospheric Doppler Radar Wind Profiler (TDRWP) at Cape Canaveral and a radiosonde comparative study at the National Weather Service (NWS) Sterling Field Support Center. Crucially, the TDRWP offers one of the most comparative wind measurements to a HALAS system due to the identical technological methodology: a line-of-sight-based, time-of-flight doppler measurement. The HALAS ground system and TDRWP showed excellent agreement during co-located and simultaneous measurements as shown in Figure 11. These are further supported by the agreement to nearby radiosondes.

Figure 11: Wind measurement performance from a Cape Canaveral test campaign in Q4 2022 with the upgraded SN2 HALAS system

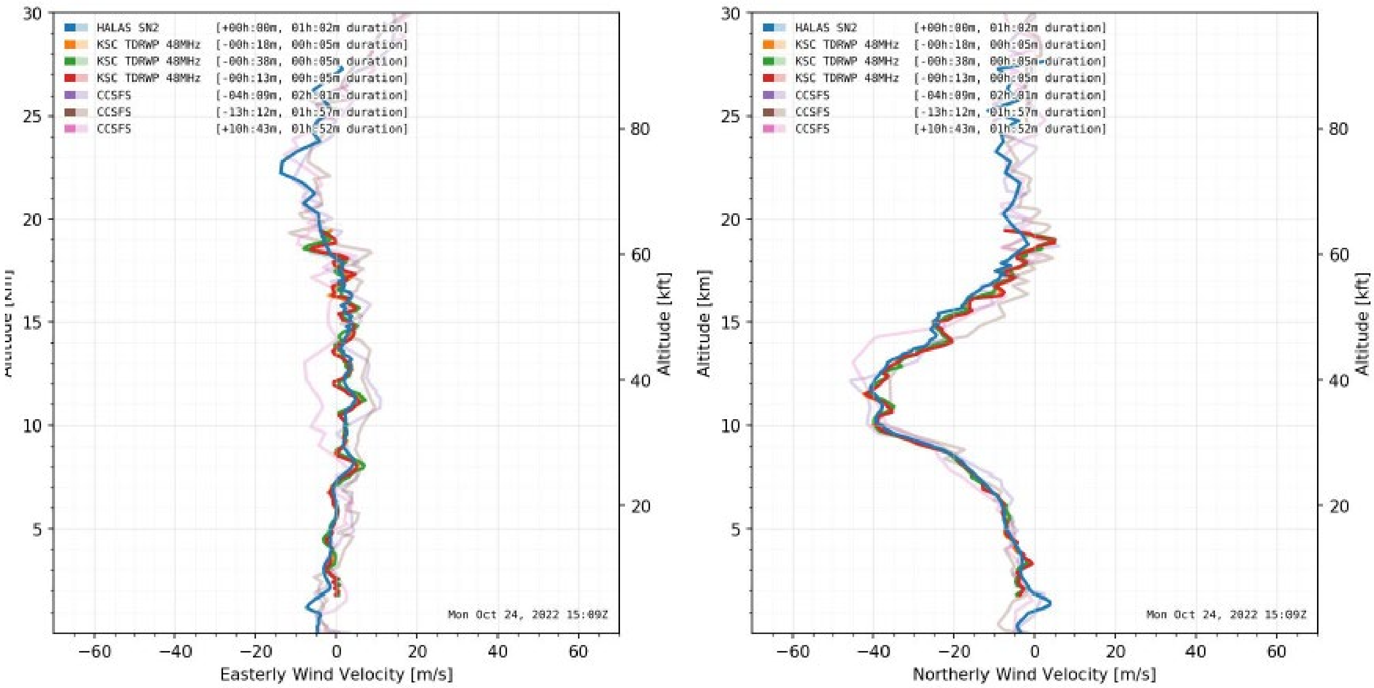

The NWS radiosonde comparison study further characterized the comparison between the HALAS ground system and local radiosondes by quantifying the difference between the two measurements. In this quantification in Figure 12, <1 m/s mean bias was calculated between measurements and <5 m/s random deviations were observed over the course of the study. Importantly, these random biases may have several causes including the random errors in both measurement techniques. There is also some bias due to different wind profiles in time and space being compared in this study (i.e., the radiosonde travels tens of kilometers during its 1–2-hour ascent and is not measuring the same volume of air as fixed scanning HALAS system). This leads to some errors from poor spatial or temporal overlap resulting in some expected random error. These general results of HALAS bias from comparisons with radiosondes were confirmed in a study of the same datasets completed by the University of Maryland, Baltimore County and supported by NOAA.

Figure 12: Total Bias from HALAS wind measurements minus radiosonde wind measurements from 3-month campaign at NWS Sterling.

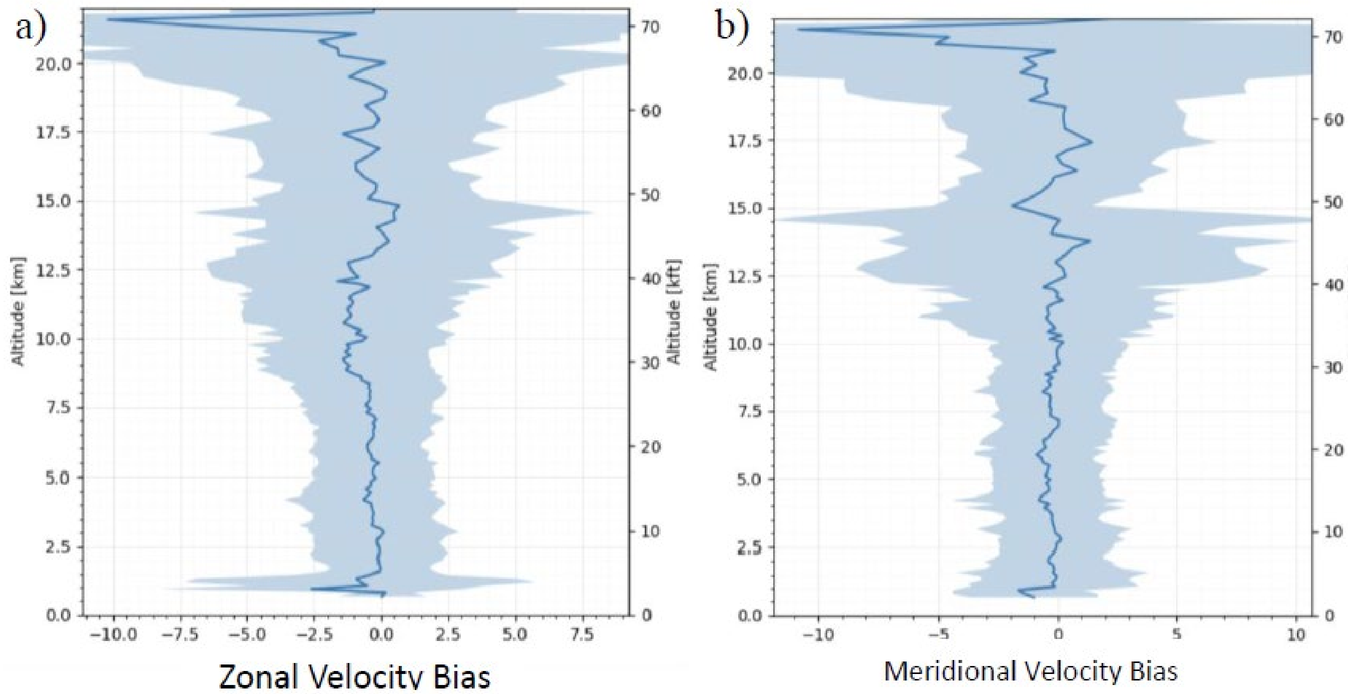

4.2 Nominal Temperature Measurement

Atmospheric temperature is measured directly from the rotational Raman spectrum detection channel on spectrometer. A typical measurement is shown in Figure 13 in which there is good agreement with nearby radiosondes. The temperature measurement is a background-limited measurement, meaning that depending upon the solar background levels the measurement performance and maximum altitude are affected. Specifically, daytime measurements are limited to 18 km in altitude while nighttime measurements can reach up to 30 km. Like with the wind measurement, the vertical resolution of the temperature measurement is varied as signal strength reduces at higher altitudes with 250 m below 10 km, 500 m below 15 km, and 1 km below 30 km. The daytime uncertainty is <1 K below 10 km and <5 K below 18 km while the nighttime uncertainty is <1 K below 18 km and <5 K below 30 km.

Figure 13: HALAS temperature measurement as a function of altitude at National Weather Service (NWS) Sterling Field Support Center in April 2024 with reference radiosondes.

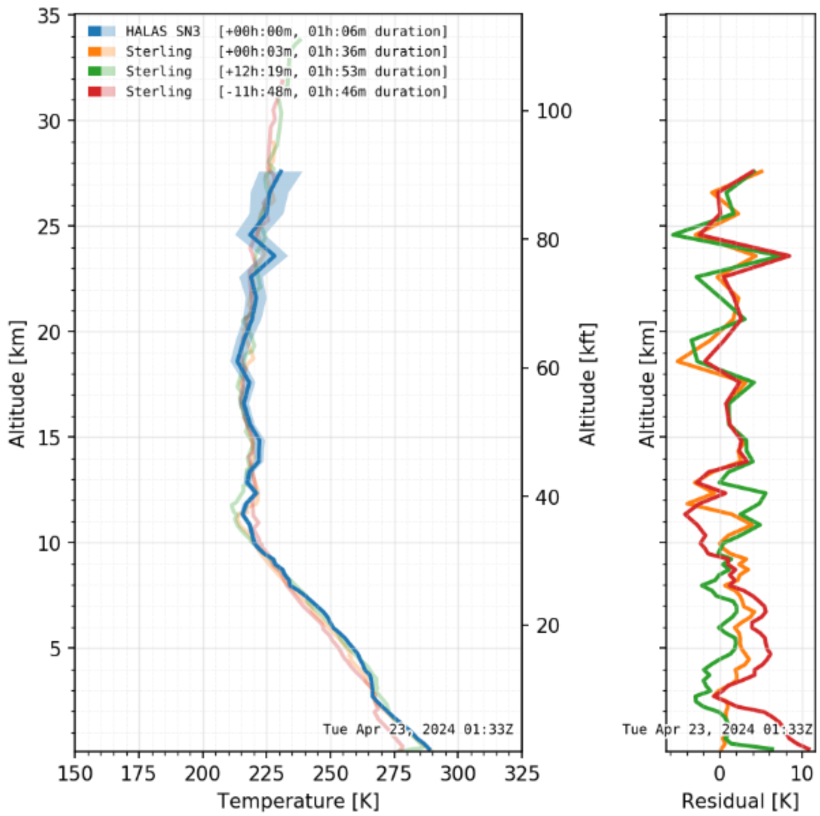

4.3 Baseline Satellite Performance

Atmospheric density measurements result from a combination of measurements. Specifically, below an altitude of interest the hydrostatic density is derived from the direct temperature measurement and above that altitude of interest a Klett inversion is used to calculate density from the elastic signal. This altitude of interest is typically ~15 km, meant to ensure that the elastic signal is free from aerosol contaminants so the proportionality between signal strength and density is well understood. A typical density measurement is shown in Figure 14 with good agreement with nearby radiosondes for altitudes available for comparison which are below the maximum balloon altitude where the radiosonde burst.

Figure 14: HALAS density measurements as a function of altitude at NWS Sterling Field Support Center in May 2024 with reference radiosondes

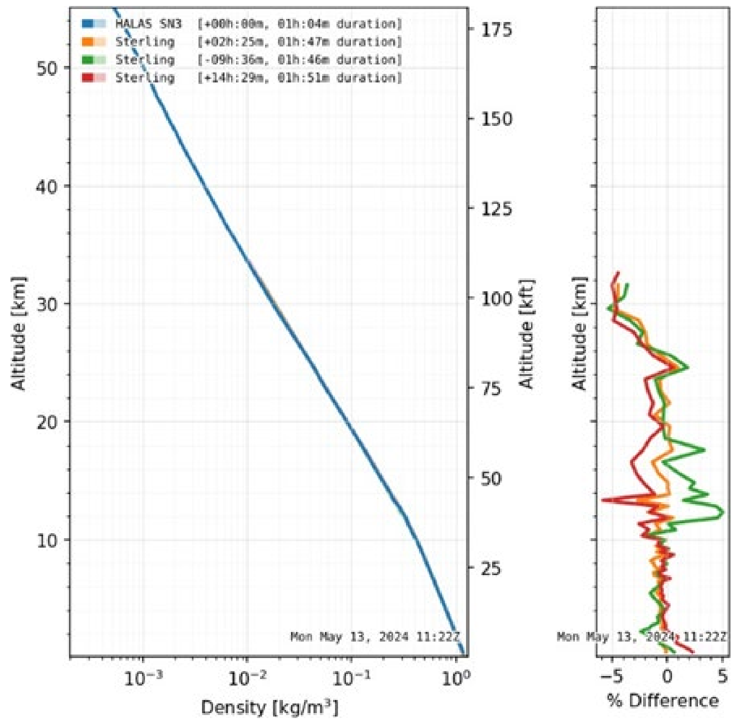

The density measurement is also a background-limited measurement with maximum altitude depending upon the time of day. Daytime measurements are limited to 40 km with <2.5% uncertainty while the upper limit is to 60 km with <2% uncertainty at nighttime. Since the low-altitude density is derived from the temperature measurement density and temperature typically share vertical resolutions except density has a higher vertical range up to 60 km for the 1-km vertical resolution bins.

4.4 Nominal Humidity Measurement

Atmospheric humidity measurements include absolute humidity, relative humidity, mixing ratio, and dew point. This measurement relies on multiple data products including temperature and density and with water vapor content derived from the detection of vibrational Raman water and nitrogen channels. A typical humidity dataset is seen in Figure 15 below showing excellent agreement with colocalized and co-temporal radiosondes. It is worthwhile to note that due to the high spatial and temporal variability of this measurement the agreement with radiosondes is often difficult to ascertain.

Figure 15: HALAS absolute humidity measurement as a function of altitude at NWS Sterling Field Support Center in (a) April 2024 and (b) May 2024 with reference radiosondes.

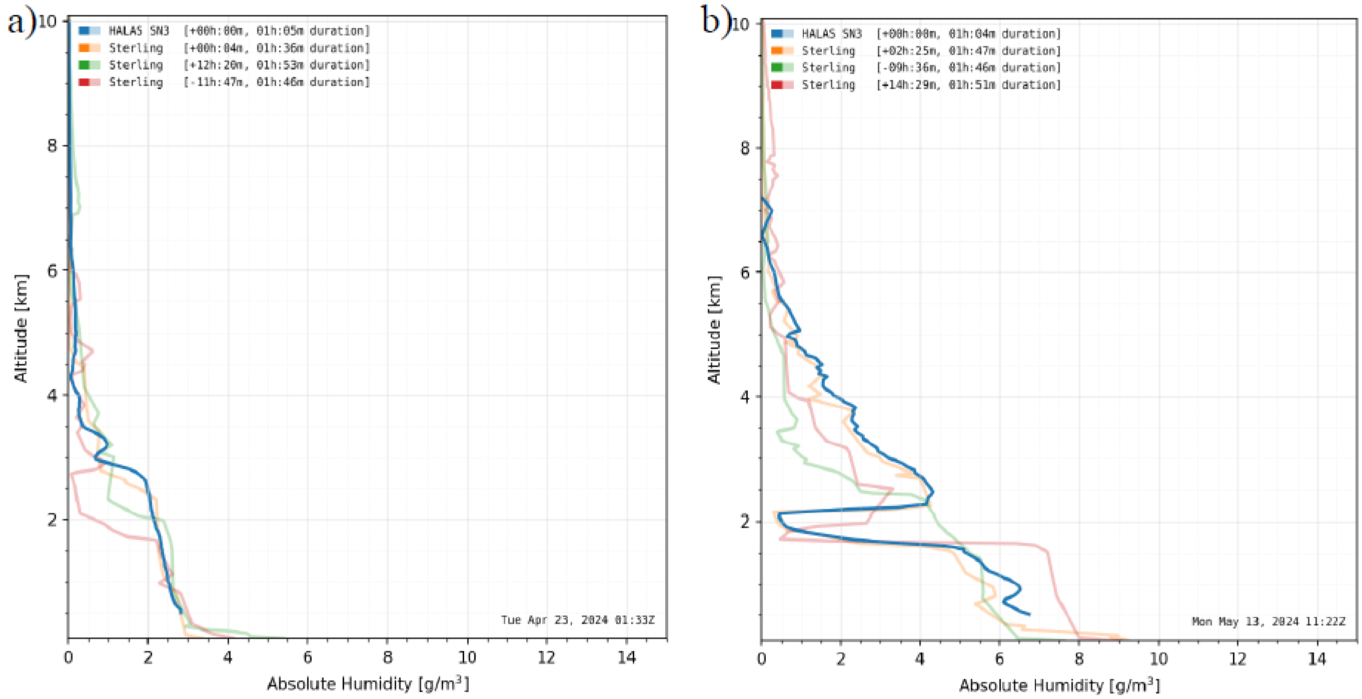

The humidity measurement is highly dependent on solar loading giving different daytime and nighttime maximum altitudes. Daytime measurements are limited to 4 km and nighttime measurements reach a maximum of 10 km. The detection limits are difficult to define agnostic of the atmospheric moisture level, however, a mixing ratio of 0.2 g/kg during the day and 0.03 g/kg during nighttime measurements are typical.

4.5 Future Improvements and Atmospheric Data Products

The standard suite of atmospheric quantities (wind, temperature, density, and humidity) is typical of most atmospheric measurements of the HALAS ground system. Additional atmospheric information is also available but less mature. These data products include:

- Wind measurements such as wind shear
- Temperature measurements such as hydrostatic temperature to provide high-altitude temperature measurements.
- Aerosol and particulate measurements including cloud height and aerosol loading.
- Atmospheric optical properties include scattering and attenuation of molecules and aerosols and optical turbulence.

5. Considerations for Operational Capabilities and Performance

There are numerous conditions affecting a lidar-based atmospheric weather measurement. HALAS data quality depends upon several factors: 1) data-collection configuration, 2) analysis post-processing settings, and 3) atmospheric conditions. These are discussed in detail in the following sections.

5.1. Data Collection Configuration

The data-collection configuration may be altered for optimization of data products of interest. For example, wind-measurements require a diversity of lines of site to calculate the 3D wind vector whereas other data products (density, temperature, humidity, etc.) would perform better with a single vertical line-of-sight. Optimal wind measurements include line-of-sight orientations from the full 360° range in azimuth at an elevation angle of approximately 60° due to signal to background considerations. Changing lines of sight, however, reduces data collection times with time spent on moving the system. The lower elevation angle also limits maximum altitude since reaching the same altitude necessitates a longer measurement range. Therefore, wind measurements are made at the cost of small performance reduction of other data products.

Another consideration for data-collection configuration is the data need for measurement localization both in laterally (latitude and longitude) and vertically (altitude). Due to the static nature of HALAS ground systems, the ability to laterally localize a measurement is limited to a time-consuming 2–3-day relocation time or pointing the instrument towards an area of interest. Pointing the instrument towards an area of interest is limited to a small cone around the ground system. This pointing direction of the instrument has limiting effects on the performance, for example, lower elevation angles for a more distant range decreases maximum altitude of a measurement. A reduced diversity in lines of sight hampers the determination of the wind vector. To localize measurement vertically, a change in elevation angle is the only methodology to optimize or prioritize certain altitude regions, with lower elevation angles producing better measurements at lower altitudes but reduced performance at higher altitudes with the opposite true for higher elevation angles. Importantly, wind measurements become difficult at high elevation angles due to a lack of horizontal components of the Doppler wind measurement for each line of sight.

The integration time of the measurement can change performance of the system. Longer integration times reduce uncertainty levels. Shorter data collections are hampered by fixed downtime during scanner movements or shuttering for aircraft/LCH. For example, scanner movement time can collectively add up to ~5 minutes of downtime per multi-LOS measurement. For a 1-hour data collection, this corresponds to <10% downtime, however, for a 15-minute data collection this would correspond to >30% downtime reducing performance for shorter data collections further. Importantly, finer time-resolution of atmospheric data can be achieved with post-processing of the data, however, it currently comes at the cost of increased latency of the data delivery since the data will not be processed until the entire dataset is completed. For low-latency data collections shorter data collections can be taken with reduced performance.

5.2. Analysis post-processing

Analysis of the detector data to produce atmospheric data products is performed by the onboard analysis server. The vertical resolution of each data product is configurable. Larger altitude bins can be chosen for reduced uncertainty and smaller altitude bins can be chosen for increased resolution. Similarly, time resolution can also be specified to increase or reduce temporal resolution below the typical integration time of the measurement. For example, a 1-hour data collection event can be broken into four 15-minute time resolved measurements. Of course, a wind measurement is reliant on the lines of sight taken during the data collection and cannot be broken up arbitrarily without hampering performance. Subsequent data collection events can be collated to produce a rolling average of wind measurements throughout the subsequent data collections.

5.3. Atmospheric Conditions

One of the largest unknowns for HALAS measurements revolves around the specific atmospheric conditions that the sensor measures. Different environments present more challenges than others. The laser has difficulty penetrating cloud layers so strong attenuation by clouds limits maximum range of data products, with thick clouds prevents any atmospheric measurement above those cloud layers. Thin cloud layers may limit transmittance through them reducing maximum altitude of data products. Likewise strong aerosol layers have a similar effect on maximum altitude limits of data products. More subtle effects include partly cloudy conditions which can often obscure a subset of lines of sight producing poorer wind performance. Additionally, high-altitude aerosol layers can hamper density derivation from elastic data due to aerosols contaminating the signal strength. Briefly cloudy and aerosol heavy conditions can hinder data collection and reduce performance.

Another challenging atmospheric condition is high solar background. As noted previously, the HALAS ground system measurement capabilities can change dramatically between daytime and nighttime operation for certain data products. The degree to which solar background affects different data products is dependent on the backscatter source and the detector source to generate atmospheric data. Elastic signals are the least dependent upon solar background with atmospheric LiDAR signal not typically affected until >40 km. Raman scattering, however, is weaker phenomena and as such their signals strengths have more trouble overcoming noise introduced by solar background. Rotational Raman signal typically is affected >18 km, Nitrogen vibrational Raman signals can similarly extend to ~18 km with the additional difficulty of higher solar background at higher wavelengths closer to the visible optical range. Water vibrational Raman signal suffers from a number of effects including (1) a reduced scattering efficiency, (2) substantially more complex scattering spectra limiting optical filtering efficiency to capture the full spectrum, (3) higher solar background in the visible region, (4) relatively low abundance of water in the atmosphere (compared to nitrogen or oxygen), and (5) complex and rapidly dissipating water abundance with altitude in the atmosphere. These effects limit reliable daytime water vibrational Raman measurements to below 4 km altitude. Improvements have been made to the data collection software to avoid directly collecting in areas of the sky where the sun is located to help minimize these impacts, but there is still typically a tradeoff for daytime performance in certain variables as shown in Appendix 1.The detectors also have limiting impacts on data products as well. While all the photomultiplier tube detectors have relatively low noise floors allowing for solar background to be limiting, the EMCCD camera of the interferometer has a high detector background which is a limiting factor for both daytime and nighttime operations

5.4. Comparative Analysis

The HALAS system offers several unique advantages over other atmospheric sensing technologies, making it a superior choice for a wide range of applications. Traditional weather balloons, for example, provide valuable data but are limited by their inability to offer continuous, real-time measurements. Weather balloons must be launched periodically, and their data is collected sequentially as they ascend through the atmosphere. In contrast, the HALAS system provides near real-time data with high temporal and spatial resolution capabilities, allowing for continuous monitoring of atmospheric conditions.

Another common technology is radar-based atmospheric sensing, which is effective for detecting precipitation and large-scale weather patterns but lacks the fine resolution and specificity of LiDAR-based systems. Radar systems typically operate at longer wavelengths, which limits their ability to detect small particles and fine atmospheric details. The HALAS system, with its high-pulse-energy 355 nm laser, can detect a wide range of atmospheric constituents, including aerosols, molecules, and water droplets, providing a more comprehensive and detailed atmospheric profile.

Overall, the HALAS system's ability to provide near real-time, high-resolution atmospheric data, its versatility in measuring various atmospheric parameters, and its capability for continuous monitoring make it a highly effective tool for atmospheric research, weather forecasting, and other applications. Honeywell's ongoing improvements in sensor technology, algorithms, and system architectures further enhance the system's performance and reliability, ensuring that HALAS remains at the forefront of atmospheric sensing technology.

6. Summary and Conclusions

Honeywell's HALAS technology enables the delivery of accurate, localized, and timely atmospheric data to end users for a variety of applications. All HALAS systems utilize UV direct detection LiDAR which leverages both aerosol and molecular scattering to achieve performance at altitude ranges exceeding competing remote-sensing technologies. Currently fielded HALAS systems include multiple ground-based variants housed in shipping containers and the second-generation airborne variant onboard an high altitude unmanned aircraft. All HALAS systems utilize the same underlying principles of measurement and share their core hardware and software for detecting and analyzing the returned light for evidence of the underpinning aerosol and molecular scattering. Key differences between systems are platform- and application-specific transceiver and infrastructure designed to enable measurements in a diversity of environments. The HALAS technology offers distinct advantages over competing technologies achieving wind measurement in low-aerosol environments. Honeywell has demonstrated flexibility and adaptability in deploying the HALAS core instrument technology to achieve atmospheric measurements from different platforms and for different applications.

The ground-based HALAS system and its subsystems were described in some detail in this report. It is housed in a shipping container that can be mobilized for a new deployment in 2-3 days. It fills a niche of atmospheric profiling of all key parameters (temperature, density, humidity, and winds) as a standalone technology which only radiosondes currently co-occupy. Multiple ground systems have been extensively field tested since 2014 and the most current performance characteristics are documented in Table 3 (as they relate to 3D Winds requirements for this program) and Appendix.

In addition, example data from a more recent field campaigns including at NOAA's Sterling Field Support Center is provided.

The 2nd Generation of HALAS Airborne System is an airborne HALAS LIDAR designed for high-altitude atmospheric measurements. Compared to previous HALAS airborne and ground systems the GH system is ruggedized and SWAP-improved (280 kg weight, 0.7 m3 volume, and 1 kW maximum power draw), making it a suitable candidate baseline design for future airborne or space variants. While testing of the GH HALAS system is underway, its performance and example data are not yet available. In the current plan, it is a key part of the upcoming campaign and results from its measurements will be delivered as part of the HAWCS data package.

7. References

HALAS - Honeywell Aerospace (Link).

Barnhart, S. and Gunasekaran, S., Design and Development of a Coherent Detection Rayleigh Doppler Lidar System for Use as an Alternative Velocimetry Technique in Wind Tunnels, Aug. 2020, (Link).

Mathew, G, *Characterization Of Stimulated Raman Scattering In Different Materials*, July 2015 (Link).

Veselovskii, I., Whiteman, D. N., Korenskiy, M., Suvorina, A., & Pérez-Ramírez, D. (2015). *Use of rotational Raman measurements in multiwavelength aerosol lidar for evaluation of particle backscattering and extinction.* Atmospheric Measurement Techniques, 8(10), 4111–4122 (Link).

Kim, D., & Cha, H. (2005). *Rotational Raman lidar for obtaining aerosol scattering coefficients*. Optics Letters, 30(13), 1728 (Link).

Kumar, S., Kumar, P., Das, A., & Pathak, C. S. (2020). *Surface-Enhanced Raman Scattering: Introduction and applications*. In IntechOpen eBooks, (Link).

Beck, H., & Kühn, M. (2017). *Dynamic data filtering of Long-Range Doppler LIDAR wind speed measurements. Remote Sensing*, 9(6), 561, (Link)

Liu, FC and Yi, F, Lidar-measured atmospheric N2 vibrational-rotational Raman spectra and consequent temperature retrieval, Optics Express, Vol. 22, Issue 23, pp. 27833-27844 (2014), (Link).

Wandinger, U. (2005), Raman Lidar. In C. Weitkamp (Ed.), *Lidar: Range-Resolved Optical Remote Sensing of the Atmosphere* (pp. 241-271). Springer.

8. Acronyms

Acronym	Description
ADSB	Automatic Dependent Surveillance–Broadcast
A2D	Analog to digital
CCD	Charge-coupled device
CCSFS	Cape Canaveral Space Force Station
CMOS	Complementary metal-oxide-semiconductor
COTS	Commercial off-the-shelf
EMCCD	Electron multiplying charge-coupled device
GUI	Graphical user interface
HVAC	Heating, ventilation, and air-conditioning
LCH	Laser Clearinghouse
LiDAR	Light Detection and Ranging
LOS	Line of Sight
NWS	National Weather Service
PMT	Photomultiplier tube
SNR	Signal-to-noise ratio
SWaP	Size, Weight, and Power
TDRWP	Tropospheric Doppler Radar Wind Profiler
TREX	Transmit and Receive Module
UV	Ultraviolet
1-D	One-dimensional
2-D	Two-dimensional

9. Appendix

Table 4: HALAS typical measurement performance for key data products.

	Temperature (Daytime)	Temperature (Nighttime)	Moisture (Daytime)	Moisture (Nighttime)	Wind	Density (Daytime)	Density (Nighttime)
Geographic Coverage / Horizontal Resolution*	150 m - 21 km	150 m - 35 km	600 m - 5 km	600 m - 14 km	1.5-23 km	150 m - 46 km	150 m - 69 km
Max Altitude (AGL)	18 km	30 km	4 km	8-10 km	20 km	40 km	60 km
Min Altitude (AGL)	125 m	125 m	500 m	500 m	1.3 km	125 m	125 m
Vertical Resolution	Typical: 250 m <10 km 500 m < 15 km 1 km < 40 km	Typical: 250 m <10 km 500 m < 15 km 1 km < 40 km	Typical: 50 m < 5 km 200 m < 10 km 500 m < 20 km	Typical: 50 m < 5 km 200 m < 10 km 500 m < 20 km	130 m < 12 km 260 m < 32 km	250 m <10 km 500 m < 15 km 1 km < 90 km	250 m <10 km 500 m < 15 km 1 km < 90 km
Measurement Accuracy	1 K < 10 km 5 K < 18 km	1 K < 18 km 5 K < 30 km	0.2 g/kg *mixing ratio, variable with moisture level and solar background	.03 g/kg < 5 km .01 g/kg < 10 km *mixing ratio, variable with moisture level	0.5 m/s < 10 km 2 m/s < 20 km	2.5%	2%
Sampling Interval	60 min						
Latency	15 min						

*Horizontal resolution varies with altitude.